



# Effects of CeO<sub>2</sub> addition on microstructure and cavitation erosion resistance of laser-processed Ni-WC composites

Rui Yang<sup>a,b</sup>, Ye Tian<sup>a</sup>, Nengliang Huang<sup>a</sup>, Pengfei Lu<sup>a</sup>, Hao Chen<sup>b</sup>, Hua Li<sup>a</sup>, Xiuyong Chen<sup>a,\*</sup>

<sup>a</sup> Key Laboratory of Marine Materials and Related Technologies, Zhejiang Key Laboratory of Marine Materials and Protective Technologies, Ningbo Institute of Materials Technology and Engineering, Chinese Academy of Sciences, Ningbo 315201, China

<sup>b</sup> Department of Mechanical, Materials and Manufacturing Engineering, University of Nottingham Ningbo China, 199 Taikang East Road, Ningbo 315100, China

## ARTICLE INFO

### Keywords:

Composite materials  
Laser processing  
Rare earth  
Grain refining  
Cavitation erosion

## ABSTRACT

Ni-WC metal matrix composite (MMC) with excellent cavitation erosion resistance (CER) was developed via laser-remelting to the sintered Ni-WC MMC. The robustness of the hierarchical WC lamellae contributed to the outstanding CER of the laser-remelted (LM) Ni-WC MMC, of which the relative CER was nearly twice greater than that of 316L stainless steel. Cerium dioxide (CeO<sub>2</sub>) was also added, attempting to enhance the CER of the LM Ni-WC MMC further. However, despite a refined grain structure and improved microhardness were obtained in the LM Ni-WC-CeO<sub>2</sub>, the CER was compromised due to that the modified morphology and distribution of the WC grains after the addition of CeO<sub>2</sub> were not very effective in enhancing the CER. The results indicated that the morphology and distribution of the WC particles exhibited a significant influence on the CER of materials, presenting a new aspect for studying cavitation erosion.

## 1. Introduction

Cavitation erosion (CE) is a type of wear that frequently occurs on the surface of the components exposed to high-speed fluid [1]. Applying protective coatings is a cost-effective solution that offers cavitation erosion resistance (CER) to these components. Ceramic-metallic metal matrix composite (MMC) coatings are widely used for offering CER, which exhibits good mechanical properties [2,3]. However, the phase boundary adhesion of the sprayed ceramic-metallic MMC coatings is poor. Thus, brittle detachment of hard ceramic phases followed by erosion of the exposed metallic binder phases composes a typical failure mode of the thermal-sprayed ceramic-metallic MMC coatings subjected to CE [2,3]. Nevertheless, the adhesion of phase boundary can be improved via laser treatment [4]. The molten metals can wet the hard ceramic particles during laser treatment, improving the bonding at the ceramic-metallic interface. Furthermore, the addition of rare earth elements, such as cerium (Ce) and lanthanum (La), in nickel (Ni) based laser-cladded coatings can provide refined microstructure, which improves microhardness and enhances the wear and corrosion resistance [5]. Thus, rare earth elements can be utilised to enhance CER. In this study, laser-remelting (LM) is introduced to the sintered (ST) Ni-WC MMC. The ST Ni-WC MMC presents an analogy to the thermal-sprayed

Ni-WC MMC but with precise control of the ratio of each material. Meanwhile, cerium dioxide (CeO<sub>2</sub>) is also added into the Ni-WC MMC, intending to enhance CER further.

## 2. Materials and methods

The feedstocks of Ni, WC, and CeO<sub>2</sub> were blended and fed into the mould in a vacuum hot-pressing sintering furnace. The volume ratio of the Ni and WC in the mixture was 3:1, and the CeO<sub>2</sub> was 2.7 wt% of the total weight. The specimens were sintered at 1250 °C with a 40 MPa load. The ST specimens were remelted by the laser with a power of 400 W, a spot size of 0.5 mm, and an overlapping ratio of 50% at a transverse speed of 200 mm/min in nitrogen gas. The as-remelted specimens were ground and polished. Then, the polished specimens were characterised by scanning electron microscope (SEM), X-ray diffraction (XRD) and electron backscattered diffraction (EBSD). A copper anode was used in XRD operated at 40 mA and 40 kV. In addition, Vickers hardness test was performed on the MMCs under 0.2 kgf. The CER of the laser-remelted (LM) MMCs and stainless steel 316L (316L SS) was evaluated in deionised water as per a previous study [6].

\* Corresponding author.

E-mail address: [chenxiuyong@nimte.ac.cn](mailto:chenxiuyong@nimte.ac.cn) (X. Chen).

<https://doi.org/10.1016/j.matlet.2021.131583>

Received 5 November 2021; Received in revised form 9 December 2021; Accepted 21 December 2021

Available online 24 December 2021

0167-577X/© 2021 Elsevier B.V. All rights reserved.

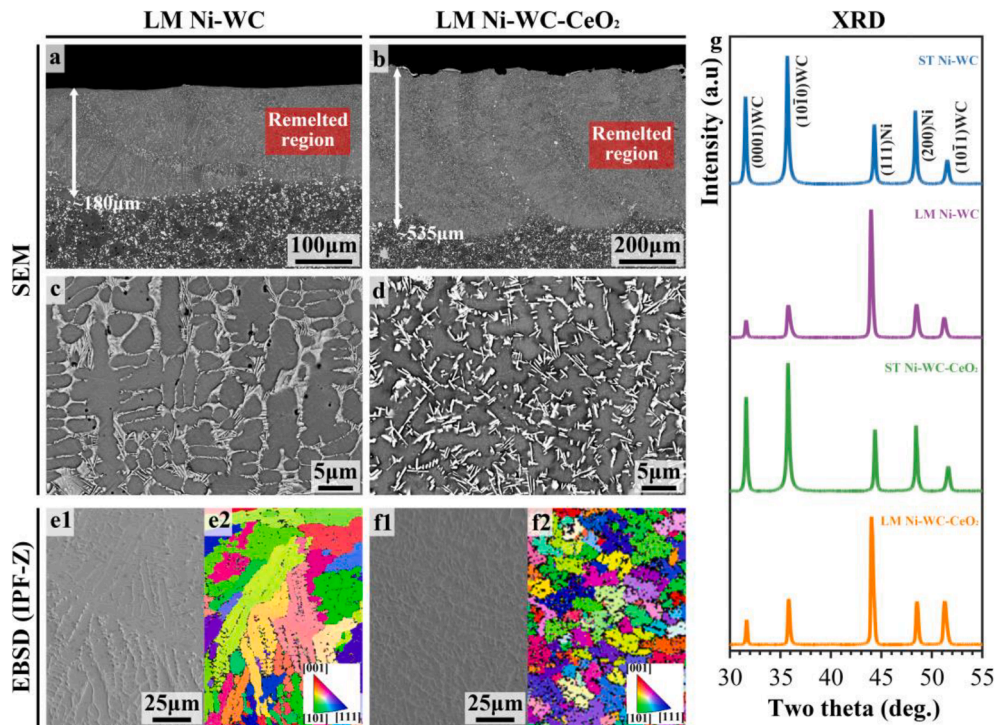


Fig. 1. SEM images (a-d) and EBSD mappings (e1&f1: SEM images, e2&f2 corresponding IPF-Z) of the LM MMCs; XRD spectra (g) of the ST and the LM MMCs.

**Table 1**  
Properties of the 316L SS and the LM MMCs.

| Specimen               | Ni grain size ( $\mu\text{m}$ ) | Microhardness ( $\text{Hv}_{0.2}$ ) | $V_{\text{loss}}$ ( $\text{mm}^3/\text{cm}^2\cdot\text{h}$ ) | $R_c$ ( $\text{h}/\text{mm}^3\cdot\text{cm}^2$ ) |
|------------------------|---------------------------------|-------------------------------------|--|--|
| 316L SS                | N/A                             | $199.8 \pm 7.0$                     | $0.19 \pm 0.01$  | $5.26 \pm 0.09$                                  |
| Ni-WC                  | $10.3 \pm 5.4$                  | $336.4 \pm 4.8$                     | $0.08 \pm 0.01$  | $11.85 \pm 0.70$                                 |
| Ni-WC-CeO <sub>2</sub> | $7.4 \pm 2.7$                   | $380.8 \pm 7.9$                     | $0.10 \pm 0.01$  | $10.45 \pm 0.40$                                 |

### 3. Results and discussion

After LM, a uniform and homogeneous remelted layer was formed (Fig. 1a&b). The increased thickness of the LM Ni-WC-CeO<sub>2</sub> could be attributed to the decreased melting temperature [7] or the improved laser absorption efficiency [8] due to the addition of CeO<sub>2</sub>. The morphologies of both LM MMCs were similar (Fig. 1c&d), presenting lamellar WC grains embedded into the Ni matrix. However, the WC lamellae in the Ni-WC-CeO<sub>2</sub> were thicker and less sharp than those in the Ni-WC. Meanwhile, the distribution of the WC lamellae in the Ni-WC-CeO<sub>2</sub> was much more homogeneous but did not form a continuous network. For the Ni-WC, Ni was segmented by the WC network, in which

the WC lamellae involved pileups, interlocked with each other, and formed a hierarchical structure. The XRD (Fig. 1g) shows that the LM MMCs only consisted of fcc Ni and hcp WC. The absence of the diffraction peaks of W<sub>2</sub>C, Ni<sub>4</sub>W, and Ce may be attributed to their low concentration. Preferred orientation was not observed in both LM MMCs according to EBSD (Fig. 1e&f). The grain size of the Ni in the LM Ni-WC-CeO<sub>2</sub> was much smaller than that in the LM Ni-WC, which was probably attributed to the increased nucleation rate by adding CeO<sub>2</sub>. The average Ni grain size of the remelted region in the Ni-WC-CeO<sub>2</sub> was reduced by 28%, and the microhardness of the LM Ni-WC-CeO<sub>2</sub> was increased by 13% (Table 1). In addition, the microhardness of the LM MMCs was much greater than that of the ST MMCs (~264 Hv<sub>0.2</sub>), which is possibly attributed to the improved phase boundary adhesion.

As a surfactant, Ce atoms are easily captured by the crystal surfaces growing at the fastest speed and can minimise the free energy of the interfaces, reducing the difference in the surface energy and the grain growth rate of each interface [9]. This ‘pinning’ effect offered improved thickness and roundness of the WC grains to the LM Ni-WC-CeO<sub>2</sub>. Apart from the promoted nucleation rate, the ‘pinning’ effect may also contribute to the refined grains [10]. In addition, the pinning effect can cause the dissolved WC particles being preferentially captured at the front of dendrite solidification, providing uniformly distributed WC in

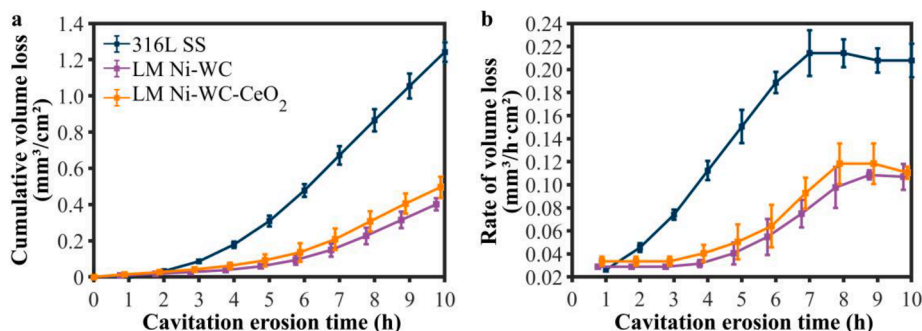
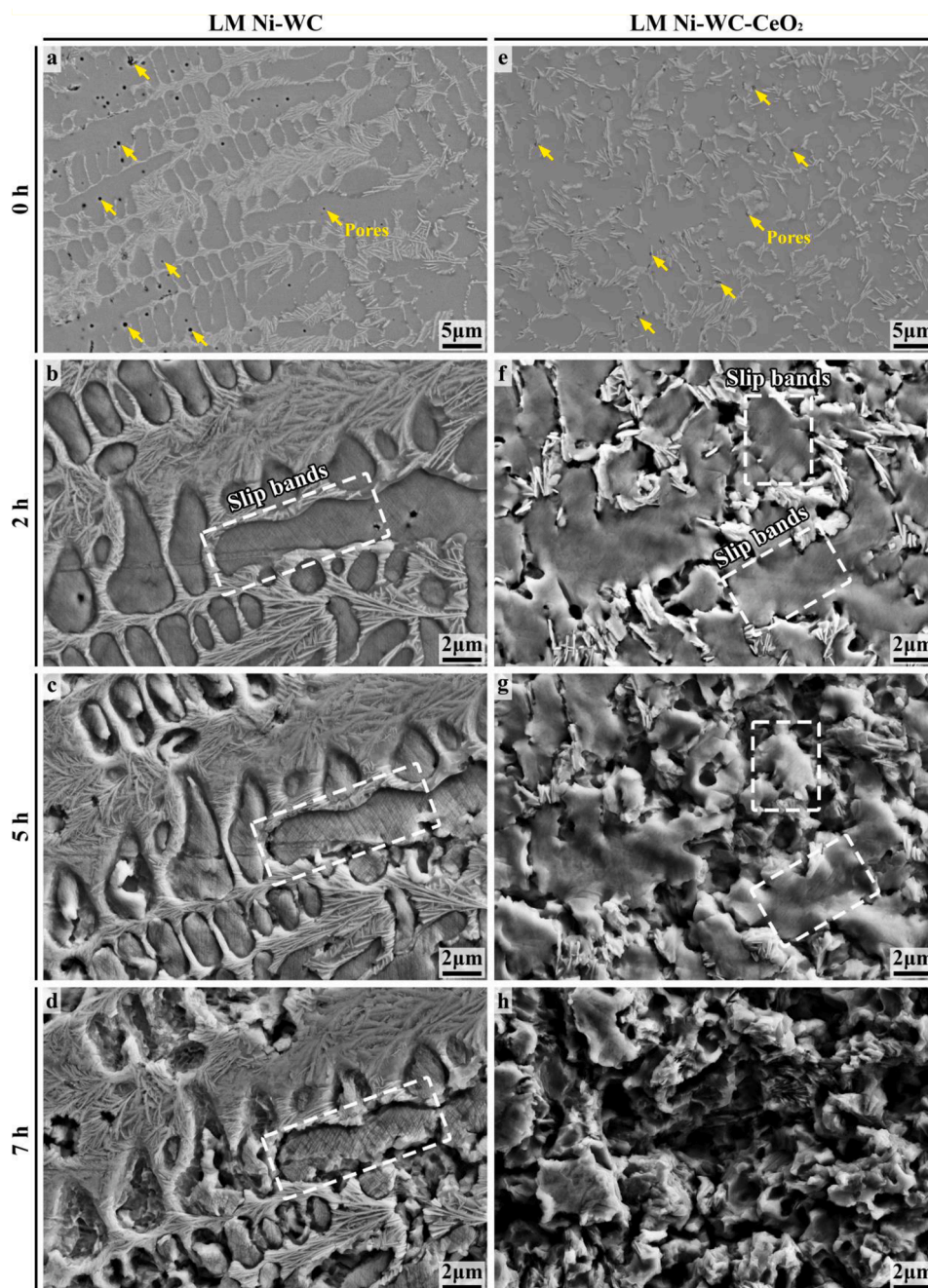


Fig. 2. Cumulative volume loss (a) and erosion rate (b) the samples.





**Fig. 3.** *In-situ* SEM observation of the LM MMCs exposed to cavitation erosion. The yellow arrows are showing the pores on the polished surface. (For interpretation of the references to colour in this figure legend, the reader is referred to the web version of this article.)

the LM Ni-WC-CeO<sub>2</sub> [10].

The CER of the LM Ni-WC-CeO<sub>2</sub> was expected to be better than that of the LM Ni-WC, as the former exhibited more uniform distribution of WC grains, more refined grains, and greater microhardness. Surprisingly, the opposite results were obtained (Fig. 2 and Table 1). The cumulative volume loss per unit area ( $V_{\text{loss}}$ ) and the rate of volume loss per unit area ( $V'_{\text{loss}}$ ) of the Ni-WC-CeO<sub>2</sub> were always greater than those of the Ni-WC. The incubation period of both MMCs was 3 h, during which the  $V'_{\text{loss}}$  was stable and less than 0.02 mm<sup>3</sup>/(cm<sup>2</sup>·h). At the 8th hour, the MMCs reached the maximum-rate period, since when the  $V'_{\text{loss}}$  has become stable again. To describe CER quantitatively, relative CER ( $R_c$ ) is used, which is defined by the time taken for the unit volume loss in the unit area at the maximum-rate period. Both LM MMCs exhibited excellent  $R_c$ , which was nearly two times greater than that of 316L SS

(Table 1).

To reveal the CE mechanism of the LM MMCs, *in-situ* SEM observation was performed (Fig. 3). There were small defects observed from the samples (highlighted by yellow arrows in Fig. 3a&e). In the first two hours (Fig. 3a-b&e-f), slip bands appeared, indicating stress accumulation by the repeated impact. As stress flow was blocked by the WC lamellae, stress concentration occurred at the phase boundaries. Thus, further impact could cause plastic deformation and material loss at the phase boundaries (Fig. 3c&f). Since then, the microstructure evolution of the two LM MMCs became different. For the Ni-WC, the material loss was almost strictly confined within each cell enclosed by the surrounding hierarchical structure of WC lamellae (Fig. 3c-d). Meanwhile, few WC lamellae were removed from the hierarchical structure during CE, even when the enclosed Ni was completely removed (Fig. 3b-d),

which was possibly attributed to the interlocking effect by the hierarchical structure of WC lamellae. Such robustness of the hierarchical structure of WC lamellae brings the excellent damage control effect to the Ni-WC subjected to CE. However, for the Ni-WC-CeO<sub>2</sub>, when WC grains were exposed, they were easily removed due to the absence of the interlocking with the WC grains nearby (Fig. 3f-g). Then, Ni was severely removed without the protection from WC grains, resulting in great material loss (Fig. 3h). This failure mode was quite similar to the other conventional thermal-sprayed WC based coatings [2,3], but the good bonding at phase boundary enabled better CER.

#### 4. Conclusions

In summary, excellent CER was achieved by LM Ni-WC(-CeO<sub>2</sub>) MMCs. The addition of CeO<sub>2</sub> reduced the Ni grain size, improved the microhardness, and provided more uniform distribution of WC grains. However, the CER of the LM Ni-WC-CeO<sub>2</sub> was reduced as the altered microstructure could not effectively resist CE. Meanwhile, the LM Ni-WC exhibited a hierarchical structure by the pileups of WC lamellae, which strictly confined the erosion within each cell, providing excellent CER. This study suggested the distribution and morphology of the WC lamellae playing a more dominant role in CER. In addition, a further investigation into the mechanism of the robustness of the hierarchical structure may benefit the design of CE resistant materials.

#### *CRedit authorship contribution statement*

**Rui Yang:** Methodology, Investigation, Writing – original draft, Writing – review & editing. **Ye Tian:** Methodology, Investigation. **Nengliang Huang:** Methodology, Investigation. **Pengfei Lu:** Methodology, Investigation. **Hao Chen:** Writing – review & editing. **Hua Li:** Writing – review & editing. **Xiuyong Chen:** Conceptualization, Supervision, Writing – review & editing.

#### Declaration of Competing Interest

The authors declare that they have no known competing financial

interests or personal relationships that could have appeared to influence the work reported in this paper.

#### Acknowledgements

This work was supported by the Zhejiang Provincial Natural Science Foundation of China (LZ22E090001), Ningbo 3315 Talents Program (2020A-29-G), Ningbo Natural Science Foundation Programme (2019A610176), and Natural Science Foundation of China (51901107), National Key Lab Fund (JCKY61420052013).

#### References

- [1] B.K. Sreedhar, S.K. Albert, A.B. Pandit, Cavitation damage: Theory and measurements – A review, *Wear* 372–373 (2017) 177–196.
- [2] L. Thakur, N. Arora, A study on erosive wear behavior of HVOF sprayed nanostructured WC-CoCr coatings, *J. Mech. Sci. Technol.* 27 (5) (2013) 1461–1467.
- [3] S. Hong, Y. Wu, J. Zhang, Y. Zheng, Y. Qin, J. Lin, Ultrasonic cavitation erosion of high-velocity oxygen-fuel (HVOF) sprayed near-nanostructured WC-10Co-4Cr coating in NaCl solution, *Ultrason. Sonochem.* 26 (2015) 87–92.
- [4] C.T. Kwok, H.C. Man, F.T. Cheng, K.H. Lo, Developments in laser-based surface engineering processes: with particular reference to protection against cavitation erosion, *Surf. Coat. Technol.* 291 (2016) 189–204.
- [5] K.L. Wang, Q.B. Zhang, M.L. Sun, X.G. Wei, Y.M. Zhu, Microstructure and corrosion resistance of laser clad coatings with rare earth elements, *Corros. Sci.* 43 (2) (2001) 255–267.
- [6] H. Zhang, Y. Gong, X. Chen, A. McDonald, H. Li, A comparative study of cavitation erosion resistance of several HVOF-sprayed coatings in deionized water and artificial seawater, *J. Therm. Spray Technol.* 28 (5) (2019) 1060–1071.
- [7] L. Chen, Y.u. Zhao, C. Guan, T. Yu, Effects of CeO<sub>2</sub> addition on microstructure and properties of ceramics reinforced Fe-based coatings by laser cladding, *Int. J. Adv. Manuf. Technol.* 115 (7-8) (2021) 2581–2593.
- [8] Y.A. Liu, R.L. Sun, W. Niu, T.G. Zhang, Y.W. Lei, Effects of CeO<sub>2</sub> on microstructure and properties of TiC/Ti<sub>2</sub>Ni reinforced Ti-based laser cladding composite coatings, *Opt. Lasers Eng.* 120 (2019) 84–94.
- [9] Y.S. Tian, C.Z. Chen, L.X. Chen, Q.H. Huo, Effect of RE oxides on the microstructure of the coatings fabricated on titanium alloys by laser alloying technique, *Scr. Mater.* 54 (5) (2006) 847–852.
- [10] D.a. Shu, S. Dai, G. Wang, W. Si, P. Xiao, X. Cui, X.u. Chen, Influence of CeO<sub>2</sub> content on WC morphology and mechanical properties of WC/Ni matrix composites coating prepared by laser in-situ synthesis method, *J. Mater. Res. Technol.* 9 (5) (2020) 11111–11120.